Fundamental frequency analysis of rectangular piezoelectric nanoplate under in-plane forces based on surface layer, non-local elasticity, and two variable refined plate hypotheses

Leila Jamali[1,2], *Aazam Ghassemi*[1,2] ✉

[1]*Department of Mechanical Engineering, Najafabad Branch, Islamic Azad University, Najafabad, Iran*
[2]*Modern Manufacturing Technologies Research Center, Najafabad Branch, Islamic Azad University, Najafabad, Iran*
✉ *E-mail: a_ghassemi@pmc.iaun.ac.ir*

Published in Micro & Nano Letters; Received on 14th June 2017; Revised on 16th July 2017; Accepted on 28th July 2017

Fundamental frequency analysis of rectangular piezoelectric nanoplates via the surface layer and non-local small-scale hypotheses is investigated in the present work. The piezoelectric nanoplate is under in-plane forces. The equilibrium governing of piezoelectric nanoplates is attained via the two variable refined plate hypothesis, and then the equations of motion are achieved utilising Hamilton's principle. To solve these equations, the finite difference method is employed. To verify the exactness of the finite difference method, the governing equations are tested by the Navier's solution. Numerical results show a good accuracy among the outcomes of the present work and some accessible cases in the literature. The numerical results show that for negative residual surface stress, as the boundary condition becomes stiffer the effect of surface layer increases, while for positive one that phenomenon is inverse.

1. Introduction: In recent years, nanoelectromechanical systems (NEMSs) have been utilised to create diverse smart equipment due to their inherent electromechanical influences such as actuators, sensors, harvesters, resonators, transducers, narrow band filtering, mass and force detection, atomic force microscopes, and so on. Thanks to their inherent characteristics, NEMSs have brought about a huge attention owing to their potential requests and excellent physical attributes in current technology and science [1].

The classical continuum hypothesis neglects the influences of the dependence of material traits and small scale in nanosize structures. Therefore, including the small-scale effects has been recommended by Eringen and Edelen [2]. Eringen developed the non-local hypothesis in the continuum models for precise prediction of mechanical behaviours of nanosize structures. The non-local hypothesis is via this presumption that the stress at a reference point is included as a purpose of the strain field at all reference points in the continuum mass.

Since the nanostructures have the high proportion of the surface to volume, the surface stress effects have an important role in their mechanics behaviour of these structures. The effect of the residual surface stress on the nanostructures gives the distributed loading on the two surfaces. Hence, Gurtin and Murdoch [3] have considered surface stress effects. In this theory, the surface is considered as a part of the two-dimensional body with zero thickness which has covered the total volume.

There are many theories to derive structural equation of piezoelectric and graphene nanoplate. Therefore, the piezoelectric nanostructures and graphene sheets have been investigated via classical plate hypothesis [4–8], first-order shear deformation hypothesis [9–11]. While few efforts were also conducted to examine both the influences of non-local elasticity and the surface layer on the piezoelectric nanosize structures via refined plate hypothesis. It has been indicated that the examination of vibration of nanoplates completely relates to the implemented plate hypothesis. The two variable refined plate hypothesis was introduced by Shimpi [12]. This hypothesis has a strong analogy with the classical plate theory, in terms of some equations and expressions. Moreover, in contrast to first-order shear deformation hypothesis, there is not a shear coefficient. Therefore, recently, some scholar derived the governing equations of graphene sheets via refined plate theory [13–16].

In recent years, Farajpour *et al.* [17] studied the vibration of piezoelectric nanofilm via electromechanical sensors based on higher-order strain gradient and non-local theories. They indicated that the frequency shifts of piezoelectric nanofilm could enhance or diminish depending on the values of small-scale parameters. In addition, Nazemizadeh and Bakhtiari-Nejad [18] analysed the size-dependent free vibration of nano and microbeams with piezo-layered actuators utilising classical plate theory. They found that the non-local parameter, length ratio, and thickness ratio have profound impacts on the free vibration of systems. In these papers [17, 18], the surface energy effect is not considered.

None of the above researchers has included refined plate theory to investigate the influences of the surface layers (the surface elasticity, surface density, and residual surface stress), non-local effect, and in-plane forces on the fundamental frequency of rectangular piezoelectric nanoplate. Owing to the importance of effects of the surface layer, small scale, and refined plate hypothesis, analysing the fundamental frequency behaviour of piezoelectric nanoplates can be included as a powerful scientific need and its investigation seems to be essential.

In the current work, an effort has been made to study the natural frequency of piezoelectric nanoplates via refined plate theory. To include the non-local and surface layer influences on the piezoelectric nanoplates, the Eringen's non-local elasticity, and Gurtin–Murdoch's theories are implemented. On the top and bottom of nanoplate, two similar surface layers are covered. Utilising Hamilton's principle, the governing equations are attained for the free vibration of the piezoelectric nanoplates. To solve the equations, the finite difference method is employed. The governing equations are solved by the Navier's solution for validating the precision of the finite difference solution. These numerical results can be a criterion for future investigation of piezoelectric nanoplate. The emphasis of the current survey is via studying the influences of diverse parameters such as the mechanical and electrical in-plane forces, nanoplate thickness, aspect ratio, residual surface stress, non-local parameter, boundary condition, and biaxial and uniaxial in-plane loading.

2. Formulation: The formation of the problem is indicated in Fig. 1. The piezoelectric nanoplate has length l_x, width l_y, thickness h, and surface layers $s^{\pm}$. The materials of piezoelectric are presumed uniform. It is presumed that the upper and lower of piezoelectric nanoplate are under the equal external electric voltage, V_0. According to the non-local piezoelectricity hypothesis, the tension tensor and the electric displacement at a material point relied not only on the strain and electric-field components at an equal place but also on all other points of the mass. Therefore, for the piezoelectric material, the non-local equivalent differential constitutive equations can be as follows [2]:

$$\begin{aligned}(1-(e_0a)^2\nabla^2)\sigma_{ij} &= C_{ijkl}\varepsilon_{kl} - e_{kij}\boldsymbol{E}_k \\ (1-(e_0a)^2\nabla^2)\boldsymbol{D}_i &= e_{ikl}\varepsilon_{kl} - \kappa_{kij}\boldsymbol{E}_k\end{aligned} \tag{1}$$

where σ_{ij}, ε_{ij}, $\boldsymbol{E}_i$, and $\boldsymbol{D}_i$ are, respectively, the components of the non-local stress tensor, strain tensor, electric-field vector, and electric displacement vector. In addition, c_{ijkl}, κ_{kij}, and e_{kij} are, respectively, the components of a fourth-order elasticity tensor, dielectric constants, and piezoelectric constants. ∇^2 is the Laplace operator and also e_0a is the non-local parameter. Using the Hamilton's principle, the governing equations of motion for the piezoelectric nanoplate are derived as follows [19, 20]:

$$\begin{aligned}&\frac{\partial^2 M^b_{xx}}{\partial x^2} + 2\frac{\partial^2 M^b_{xy}}{\partial x\partial y} + \frac{\partial^2 M^b_{yy}}{\partial y^2} + 2\tau^s\nabla^2(w^b+w^s) \\ &\quad + \left(N_{xm}+N_{xe}\right)\frac{\partial^2(w^b+w^s)}{\partial x^2} + \left(N_{ym}+N_{ye}\right)\frac{\partial^2(w^b+w^s)}{\partial y^2} \\ &\quad = m_0\left(\frac{\partial^2 w^b}{\partial t^2}+\frac{\partial^2 w^s}{\partial t^2}\right) - m_2\left(\frac{\partial^4 w^b}{\partial t^2\partial x^2}+\frac{\partial^4 w^b}{\partial t^2\partial y^2}\right) \\ &\frac{\partial^2 M^s_{xx}}{\partial x^2} + 2\frac{\partial^2 M^s_{xy}}{\partial x\partial y} + \frac{\partial^2 M^s_{yy}}{\partial y^2} + \frac{\partial Q_{xz}}{\partial x} + \frac{\partial Q_{yz}}{\partial y} \\ &\quad + 2\tau^s\nabla^2(w^b+w^s) + \left(N_{xm}+N_{xe}\right)\frac{\partial^2(w^b+w^s)}{\partial x^2} \\ &\quad + \left(N_{ym}+N_{ye}\right)\frac{\partial^2(w^b+w^s)}{\partial y^2} \\ &\quad = m_0\left(\frac{\partial^2 w^b}{\partial t^2}+\frac{\partial^2 w^s}{\partial t^2}\right) - \frac{m_2}{84}\left(\frac{\partial^4 w^s}{\partial t^2\partial x^2}+\frac{\partial^4 w^s}{\partial t^2\partial y^2}\right)\frac{\partial D_z}{\partial z} = 0\end{aligned} \tag{2}$$

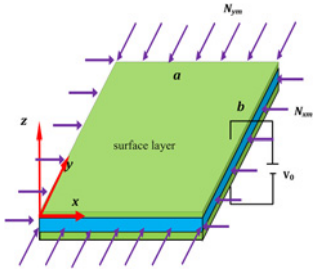

Fig. 1 *Symbolic of the piezoelectric nanoplate considering the surface layers*

where (N_{xm}, N_{xe}) and (N_{ym}, N_{ye}) are the electric and mechanical forces for the x and y directions, respectively. $M_{\alpha\beta}$ and $Q_{\alpha\beta}$ are, respectively, the bending moment and shear forces. Thus, the resultant stresses are introduced as

$$\begin{aligned}M^b_{\alpha\beta} &= \int_{-h/2}^{h/2} z\sigma^b_{\alpha\beta}\mathrm{d}z + (\sigma^{b,s+}_{\alpha\beta} - \sigma^{b,s-}_{\alpha\beta})\frac{h}{2} \quad \alpha,\ \beta = x,\ y \\ M^s_{\alpha\beta} &= \int_{-h/2}^{h/2}\left(-\frac{1}{4}z + \frac{5}{3}z\left(\frac{z}{h}\right)^2\right)\sigma^s_{\alpha\beta}\,\mathrm{d}z \\ &\quad + (\sigma^{s,s+}_{\alpha\beta} - \sigma^{s,s-}_{\alpha\beta})\frac{h}{2} \quad \alpha,\ \beta = x,\ y \\ Q_{\alpha z} &= \int_{-h/2}^{h/2}\sigma_{\alpha z}\,\mathrm{d}z + (\sigma^{s+}_{\alpha z} + \sigma^{s-}_{\alpha z}) \quad \alpha = x,\ y\end{aligned} \tag{3}$$

m_0 and m_2 are the mass inertias introduced as

$$(m_0,\ m_2) = \int_{-h/2}^{h/2}\rho(1,\ z^2)\,\mathrm{d}z \tag{4}$$

The electric field is taken to be present only in the z-direction ($E_x = E_y = 0$), and it is pertained to the electric potential φ by

$$E_z = -\frac{\partial\varphi}{\partial z} \tag{5}$$

where ρ is the mass density of the piezoelectric nanoplate. By using (1), (5) and electric boundary conditions $\phi(h/2) = V_0$, $\phi(-h/2) = 0$, the electric potential ϕ can be achieved as

$$\begin{aligned}\phi = &-\frac{e_{31}}{2\kappa_{33}}\left\{\left(z^2-\frac{h^2}{4}\right)\nabla^2 w^b + \left[-\frac{1}{4}z^2 + \frac{5}{6}z^2\left(\frac{z}{h}\right)^2 + \frac{h^2}{96}\right]\nabla^2 w^s\right\} \\ &+ \frac{V_0}{h}z + \frac{V_0}{2}\end{aligned} \tag{6}$$

Using (5), (6), the electric field is obtained as follows:

$$E_z = \frac{e_{31}}{\kappa_{33}}\left(z\nabla^2 w^b + \left[-\frac{1}{4}z + \frac{5}{3}z\left(\frac{z}{h}\right)^2\right]\nabla^2 w^s\right) - \frac{V_0}{h} \tag{7}$$

Therefore, the bending and shearing electric field is stated as follows:

$$\begin{aligned}E^b_z &= \frac{e_{31}}{\kappa_{33}}\left(z\nabla^2 w^b\right) - \frac{V_0}{2h}, \\ E^s_z &= \frac{e_{31}}{\kappa_{33}}\left(\left[-\frac{1}{4}z + \frac{5}{3}z\left(\frac{z}{h}\right)^2\right]\nabla^2 w^s\right) - \frac{V_0}{2h}\end{aligned} \tag{8}$$

doi: 10.1049/mnl.2017.0429

Based on reference [19, 20], the stress resultants are written in terms of the displacement components as follows:

$$N_{xm}=N,\quad N_{ym}=N,\quad \text{(for biaxial in-plane force)}$$

$$N_{xm}=N,\quad N_{ym}=0,\quad \text{(for uniaxial in-plane force)}$$

$$N_{xe}=N_{ye}=e_{31}V_0$$

$$\begin{Bmatrix} M^b_{xx}\\ M^b_{yy}\\ M^b_{xy}\end{Bmatrix}-(e_0a)^2\nabla^2\begin{Bmatrix} M^b_{xx}\\ M^b_{yy}\\ M^b_{xy}\end{Bmatrix}=\begin{bmatrix} D^b_{11} & D^b_{12} & 0\\ D^b_{12} & D^b_{22} & 0\\ 0 & 0 & D^b_{66}\end{bmatrix}\begin{Bmatrix} -\partial^2 w^b/\partial x^2\\ -\partial^2 w^b/\partial y^2\\ -2\partial^2 w^b/\partial x\partial y\end{Bmatrix}$$

$$\begin{Bmatrix} M^s_{xx}\\ M^s_{yy}\\ M^s_{xy}\end{Bmatrix}-(e_0a)^2\nabla^2\begin{Bmatrix} M^s_{xx}\\ M^s_{yy}\\ M^s_{xy}\end{Bmatrix}=\begin{bmatrix} D^s_{11} & D^s_{12} & 0\\ D^s_{12} & D^s_{22} & 0\\ 0 & 0 & D^s_{66}\end{bmatrix}\begin{Bmatrix} -\partial^2 w^s/\partial x^2\\ -\partial^2 w^s/\partial y^2\\ -2\partial^2 w^s/\partial x\partial y\end{Bmatrix} \tag{9}$$

$$\begin{Bmatrix} Q_{yz}\\ Q_{xz}\end{Bmatrix}-(e_0a)^2\nabla^2\begin{Bmatrix} Q_{yz}\\ Q_{xz}\end{Bmatrix}=\begin{bmatrix} D^s_{44} & 0\\ 0 & D^s_{55}\end{bmatrix}\begin{Bmatrix} \partial w^s/\partial y\\ \partial w^s/\partial x\end{Bmatrix}$$

where

$$D^b_{11}=\frac{h^3}{12}\left(C_{11}+\frac{e^2_{31}}{\kappa_{33}}+\frac{6}{h}\left[C^s_{11}+\frac{e^s_{31}e_{31}}{\kappa_{33}}\right]\right),$$

$$D^b_{22}=\frac{h^3}{12}\left(C_{22}+\frac{e^2_{31}}{\kappa_{33}}+\frac{6}{h}\left[C^s_{22}+\frac{e^s_{31}e_{31}}{\kappa_{33}}\right]\right)$$

$$D^b_{12}=\frac{h^3}{12}\left(C_{12}+\frac{e^2_{31}}{\kappa_{33}}+\frac{6}{h}\left[C^s_{12}+\frac{e^s_{31}e_{31}}{\kappa_{33}}\right]\right),$$

$$D^b_{66}=\frac{h^3}{12}\left(C_{66}+\frac{6}{h}C^s_{66}\right)$$

$$D^s_{11}=\frac{h^3}{84\times 12}\left(C_{11}+\frac{e^2_{31}}{\kappa_{33}}+\frac{84}{h}\left[C^s_{11}+\frac{e^s_{31}e_{31}}{\kappa_{33}}\right]\right),$$

$$D^s_{22}=\frac{h^3}{84\times 12}\left(C_{22}+\frac{e^2_{31}}{\kappa_{33}}+\frac{84}{h}\left[C^s_{22}+\frac{e^s_{31}e_{31}}{\kappa_{33}}\right]\right)$$

$$D^s_{12}=\frac{h^3}{84\times 12}\left(C_{12}+\frac{e^2_{31}}{\kappa_{33}}+\frac{84}{h}\left[C^s_{12}+\frac{e^s_{31}e_{31}}{\kappa_{33}}\right]\right),$$

$$D^s_{66}=\frac{h^3}{84\times 12}\left(C_{66}+\frac{84}{h}C^s_{66}\right)$$

$$D^s_{44}=\frac{5h}{6}C_{44}+2\tau^s,$$

$$D^s_{55}=\frac{5h}{6}C_{55}+2\tau^s \tag{10}$$

c_{ijkl}, κ_{kij}, and e_{kij} are, respectively, the components of a fourth-order elasticity tensor, dielectric constants, and piezoelectric constants. C^s_{ij}, e^s_{ij}, and τ^s are, respectively, the surface elastic constant, piezoelectric constant, and residual surface tension. s^+ and s^- are the surface layers for upper and lower of a nanoplate, respectively. Given the fact that the vibration response is harmonic, the deflection owing to the vibrations of thin nanoplates are mentioned by

$$w^b(x,\ y,\ t)=W^b(x,\ y)e^{i\omega t},\quad w^s(x,\ y,\ t)=W^s(x,\ y)e^{i\omega t} \tag{11}$$

where $i^2=-1$ and ω is the natural frequency. By using (2), (9), and (11), the equations of motion for the piezoelectric nanoplates are written in terms of displacements W^b and W^s as follows:

$$\begin{aligned}
&D^b_{11}\frac{\partial^4 W^b}{\partial x^4}+2(D^b_{12}+2D^b_{66})\frac{\partial^4 W^b}{\partial x^2\partial y^2}+D^b_{22}\frac{\partial^4 W^b}{\partial y^4}\\
&-2\tau^s\left\{(1-(e_0a)^2\nabla^2)\nabla^2(W^b+W^s)\right\}\\
&-(1-(e_0a)^2\nabla^2)\left\{(N_{xm}+N_{xe})\left(\frac{\partial^2 W^b}{\partial x^2}+\frac{\partial^2 W^s}{\partial x^2}\right)\right.\\
&\left.+(N_{ym}+N_{ye})\left(\frac{\partial^2 W^b}{\partial y^2}+\frac{\partial^2 W^s}{\partial y^2}\right)\right\}\\
&-\omega^2\left\{(1-(e_0a)^2\nabla^2)\left(m_0(W^b+W^s)-m_2\nabla^2(W^b)\right)\right\}=0\\
&D^s_{11}\frac{\partial^4 W^s}{\partial x^4}+2(D^s_{12}+2D^s_{66})+\frac{\partial^4 W^s}{\partial x^2\partial y^2}+D^s_{22}\frac{\partial^4 W^s}{\partial y^4}\\
&-(D^s_{55}+2\tau^s)\frac{\partial^2 W^s}{\partial x^2}-(D^s_{44}+2\tau^s)\frac{\partial^2 W^s}{\partial y^2}\\
&-2\tau^s\left\{(1-(e_0a)^2\nabla^2)\nabla^2(W^b+W^s)\right\}\\
&-\omega^2\left\{(1-(e_0a)^2\nabla^2)\left(m_0(W^b+W^s)-\frac{m_2}{84}\nabla^2(W^s)\right)\right\}\\
&-(1-(e_0a)^2\nabla^2)\left\{(N_{xm}+N_{xe})\left(\frac{\partial^2 W^b}{\partial x^2}+\frac{\partial^2 W^s}{\partial x^2}\right)\right.\\
&\left.+\left(N_{ym}+N_{ye}\right)\left(\frac{\partial^2 W^b}{\partial y^2}+\frac{\partial^2 W^s}{\partial y^2}\right)\right\}=0
\end{aligned} \tag{12}$$

3. Solution procedure

3.1. Navier's method: According to the Navier's solution, the accurate method for the free vibration of piezoelectric nanoplates, with reference to SS boundary condition can be indicated as follows:

$$\begin{aligned}
W^b&=\sum_{m=1}^{\infty}\sum_{n=1}^{\infty}W^b_{mn}\sin(\alpha x)\sin(\beta y),\\
W^s&=\sum_{m=1}^{\infty}\sum_{n=1}^{\infty}W^s_{mn}\sin(\alpha x)\sin(\beta y)
\end{aligned} \tag{13}$$

where $\alpha=m\pi/a$ and $\beta=n\pi/b$. In this case, m and n are half-wave numbers along the x and y directions. Replacing (13) into (12),

the current system of equations are attained

$$\begin{bmatrix} S_{11} & S_{12} \\ S_{21} & S_{22} \end{bmatrix} \begin{Bmatrix} W^b_{mn} \\ W^s_{mn} \end{Bmatrix} = \begin{Bmatrix} 0 \\ 0 \end{Bmatrix} \tag{14}$$

where

$$\begin{aligned}
S_{11} &= D^b_{11}\alpha^4 + 2(D^b_{12} + 2D^b_{66})\alpha^2\beta^2 + D^b_{22}\beta^4 \\
&\quad + 2\tau^s\{(\alpha^2+\beta^2) + (e_0a)^2(\alpha^2+\beta^2)^2\} \\
&\quad + (N_{xm}+N_{xe})\{\alpha^2 + (e_0a)^2(\alpha^4+\alpha^2\beta^2)\} \\
&\quad + (N_{ym}+N_{ye})\{\beta^2 + (e_0a)^2(\beta^4+\alpha^2\beta^2)\} \\
&\quad - \omega^2\rho h\{1 + (e_0a)^2(\alpha^2+\beta^2)\} \\
&\quad - \omega^2\frac{\rho h^3}{12}\{(\alpha^2+\beta^2) + (e_0a)^2(\alpha^4+\beta^4+2\alpha^2\beta^2)\} \\
S_{12} &= S_{21} = 2\tau^s\{(\alpha^2+\beta^2) + (e_0a)^2(\alpha^4+\beta^4+2\alpha^2\beta^2)\} \\
&\quad + (N_{xm}+N_{xe})\{\alpha^2 + (e_0a)^2(\alpha^4+\alpha^2\beta^2)\} \\
&\quad + (N_{ym}+N_{ye})\{\beta^2 + (e_0a)^2(\beta^4+\alpha^2\beta^2)\} \\
&\quad - \omega^2\rho h\{1 + (e_0a)^2(\alpha^2+\beta^2)\} \\
S_{22} &= D^s_{11}\alpha^4 + 2(D^s_{12} + 2D^s_{66})\alpha^2\beta^2 + D^s_{22}\beta^4 \\
&\quad + 2\tau^s\{(\alpha^2+\beta^2) + (e_0a)^2(\alpha^4+\beta^4+2\alpha^2\beta^2)\} \\
&\quad + (N_{xm}+N_{xe})\{\alpha^2 + (e_0a)^2(\alpha^4+\alpha^2\beta^2)\} \\
&\quad + (N_{ym}+N_{ye})\{\beta^2 + (e_0a)^2(\beta^4+\alpha^2\beta^2)\} \\
&\quad - \omega^2\rho h\{1 + (e_0a)^2(\alpha^2+\beta^2)\} \\
&\quad - \omega^2\frac{\rho h^3}{12\times 84}\{(\alpha^2+\beta^2) + (e_0a)^2(\alpha^4+\beta^4+2\alpha^2\beta^2)\}
\end{aligned} \tag{15}$$

The fundamental frequency is obtained under in-plane loading if the determinant of the coefficient matrix in (14) gets zero.

3.2. Finite difference method: The finite difference solution is a robust method which is implemented to solve differential equations of motion of piezoelectric nanoplates. The method substitutes the differential equations with equivalent differences equations. Fig. 2 depicts a rectangular nanoplate and the grid points which will be utilised in the finite difference solution. By implementing this method, (12) conjectures with the derivative of the transverse bending displacement, W^b, for the i, jth point as a function of its adjacent points

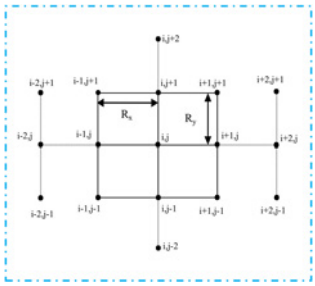

Fig. 2 *Grid points for the finite difference method*

$$\begin{aligned}
\frac{dW^b}{dx} &= \frac{1}{2R_x}(W^b_{(i+1,j)} - W^b_{(i-1,j)}), \\
\frac{dW^b}{dy} &= \frac{1}{2R_y}(W^b_{(i,j+1)} - W^b_{(i,j-1)}) \\
\frac{dW^b}{dy} &= \frac{1}{2R_y}(W^b_{(i,j+1)} - W^b_{(i,j-1)}), \\
\frac{d^2W^b}{dx^2} &= \frac{1}{R_x^2}(W^b_{(i+1,j)} - 2W^b_{(i,j)} + W^b_{(i-1,j)}) \\
\frac{d^2W^b}{dy^2} &= \frac{1}{R_y^2}(W^b_{(i,j+1)} - 2W^b_{(i,j)} + W^b_{(i,j-1)}) \\
\frac{d^4W^b}{dx^4} &= \frac{1}{R_x^4}(W^b_{(i+2,j)} - 4W^b_{(i+1,j)} + 6W^b_{(i,j)} - 4W^b_{(i-1,j)} + W^b_{(i-2,j)}) \\
\frac{d^4W^b}{dy^4} &= \frac{1}{R_y^4}(W^b_{(i,j+2)} - 4W^b_{(i,j+1)} + 6W^b_{(i,j)} - 4W^b_{(i,j-1)} + W^b_{(i,j-2)}) \\
\frac{d^4W^b}{dx^2dy^2} &= \frac{1}{R_x^2R_y^2}\begin{pmatrix} W^b_{(i+1,j+1)} + W^b_{(i-1,j+1)} + W^b_{(i-1,j-1)} + W^b_{(i+1,j-1)} + 4W^b_{(i,j)} \\ -2(W^b_{(i+1,j)} + W^b_{(i,j+1)} + W^b_{(i-1,j)} + W^b_{(i,j-1)}) \end{pmatrix}
\end{aligned} \tag{16}$$

Here, R_x and R_y are, respectively, the distance between two grid points in the x and y directions. It should be mentioned that for shear displacement the W^b converts to W^s in (16). By substituting (16) into (12) and expanding a code in MATLAB software, the equations of motion are solved.

3.3. Boundary conditions: The SS and clamped boundary conditions are investigated in this paper. These boundary conditions will be defined as follows [19, 20].

3.3.1 SS boundary condition: The SS boundary conditions are indicated as follows:

$$\frac{\partial^2 W^s}{\partial x^2} = \frac{\partial^2 W^s}{\partial y^2} = \frac{\partial^b W^b}{\partial x^2} = \frac{\partial^2 W^b}{\partial y^2} = 0 \quad W^s = W^b = 0 \tag{17}$$

3.3.2 Clamped boundary condition: The clamped boundary conditions are defined by

$$\frac{\partial W^s}{\partial x} = \frac{\partial W^s}{\partial y} = \frac{\partial W^b}{\partial x} = \frac{\partial W^b}{\partial y} = 0, \quad W^s = W^b = 0 \tag{18}$$

4. Results and discussion: This segment, the numerical simulations are performed for the case study of the Piezoelectric lead Zirconate Titanate (PZT-5H) nanoplate, with physical properties put in Table 1 [4].

Here, the accuracy and convergence of the present formulation and methods of solution are investigated through different numerical examples of piezoelectric nanoplate. Therefore, the accuracy of both Navier and finite difference solutions is demonstrated by comparing the fundamental frequency ratio of a single piezoelectric nanoplate for SS boundary condition with those of obtained by Yan and Jiang [4] in Table 2.

doi: 10.1049/mnl.2017.0429

Table 1 Physical properties of the nanoplate

$C_{11}=102$ GPa, $C_{22}=102$ GPa, $C_{12}=31$ GPa, $C_{66}=35.3$ GPa, $C_{44}=C_{55}=23$ GPa, $e_{31}=-17.05$ C/m^2, $k_{33}=1.76\times10^{-8}$ C/Vm, $C^s_{11}=7.56$ N/m, $C^s_{22}=7.56$ N/m, $C^s_{12}=3.3$ N/m, $C^s_{66}=2.13$ N/m, $e^s_{31}=-3\times10^{-8}$ C/m, $\tau^s=1$ N/m

Table 2 Comparison of the current numerical outcomes for the fundamental frequency ratio of a piezoelectric nanoplate with SS boundary condition ($l_x=l_y=20$ nm, $e_0a=0$ nm, $V_0=-0.1$ V, and $N_{xm}=N_{ym}=0$ N/m)

Solution	Theory	length to thickness ratio, l_x/h				
		40	20	10	5	2.5
[4]	Classical Plate Theory (CPT)	1.503	1.524	1.415	1.225	1.112
Finite Difference Method (FDM)	Two Variable Refined Plate Theory (TVRPT)	1.503	1.517	1.386	1.178	1.075
Navier	TVRPT	1.502	1.516	1.386	1.178	1.075

The fundamental frequency ratio is presented as follows:

$$\text{fundamental frequency ratio} = \frac{\text{fundamental frequency with surface effect}}{\text{fundamental frequency without surface effect}} \tag{19}$$

The in-plane load and non-local parameter are equal to zero. From Table 2, it can be seen that in all cases, the current results are in suitable match with those reported by Yan and Jiang [4].

To illustrate the influence of boundary conditions on the fundamental frequency of piezoelectric nanoplate, the variations of fundamental frequency ratio with the external electric voltage, aspect ratio, length to thickness ratio, and residual surface stress for various boundary conditions are plotted in Figs. 3–6, respectively. The width and small-scale coefficient of the piezoelectric nanoplate are $l_y=20$ nm and $e_0a=0.5$ nm, respectively. The effect of mechanical in-plane load is not taken into account. For briefly, six diversity boundary conditions are introduced: (i) SSSS: all borders SS; (ii) SSSC: clamped parallel with $y=b$ and SS parallel with $x=0$, $x=a$, and $y=0$; (iii) SCSC: clamped parallel with $x=a$ and $y=b$, and SS parallel with $x=0$, $y=0$; (iv) SSCC: clamped parallel with $y=0$ and $y=b$, and SS parallel with $x=0$ and $x=a$; (v) SCCC: clamped parallel with $x=a$, $y=0$, and $y=b$, and SS parallel with $x=0$; and (vi) CCCC: all borders clamped.

As seen from these figures, the non-local fundamental frequency ratios also depend strongly on the boundary conditions. When the boundary conditions get more solid, the fundamental frequency ratio decreases. Thus, the influences of surface layers reduce. Therefore, the degree of surface layers on the fundamental frequency of piezoelectric nanoplates system seems to display itself in the subsequent order of weakness: SSSS, SSSC, SCSC, SSCC, SCCC, and CCCC. Converting the boundary conditions with quite free rotations such as simply support to the boundary conditions with restraint on the rotations, e.g. clamped, the surface layer will show itself weaker. Since the surface layers have an intrinsic stiffness.

In Fig. 3, the nanoplate thickness and length are $h=1$ nm and $l_x=20$ nm. From Fig. 3, it is found that by enhancing the external electric voltages, the fundamental frequency ratio would enhance; therefore, the influence of surface layer rises. In addition, by raising that parameter to critical values the fundamental frequency of the nanoplate would get zero. It is meant that the out-of-plane plate resilient gets zero. This incident transpires sooner in lower external electric voltage for SSSS as compared with CCCC.

In Fig. 4, the nanoplate thickness and external electric voltages are $h=1$ nm and $V_0=0$ V. From Fig. 4, it can be seen that by increasing the aspect ratios, the fundamental frequency ratio would augment. Thus, the value of surface effect could enhance. Moreover, in the higher value of plate aspect ratio, the effect of boundary condition is important, since the vertical distance between curves of different boundary conditions is raised. Also, for the higher value of aspect ratio, the curves with various boundary conditions converge together. In addition, it is seen that by rising the aspect ratio to $l_x/l_y=1.5$, the surface layer effects would increase drastically, while for aspect ratio larger than 1.5, $l_x/l_y>1$, the surface energy on the fundamental frequency have no significant effects.

In Fig. 5, the nanoplate length and external electric voltages are $l_x=20$ nm and $V_0=0$ V. From Fig. 5, it is can be found that the degree of surface layers increases by augmenting length to thickness ratio. Moreover, after a critical length to thickness ratio, the influence of surface layer extremely raises. In addition, for the higher value of length to thickness ratio, the surface layer effect is more dependent on boundary condition.

In Fig. 6, the nanoplate length, thickness, and external electric voltage are $l_x=20$ nm, $h=1$ nm, and $V_0=0$ V, respectively. From this figure, it is understood that the influences of surface layers augment by enhancing the residual surface stress. Moreover, for negative residual surface stress, when the boundary condition gets

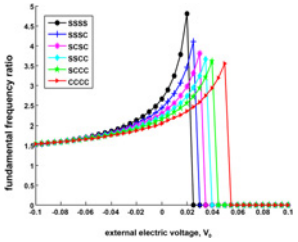

Fig. 3 *Variation of the fundamental frequency ratio with the external electric voltages of the piezoelectric nanoplate under different boundary conditions ($l_x=l_y=20$ nm, $h=1$ nm, $e_0a=0.5$ nm, $N_{xm}=N_{ym}=0$ N/m)*

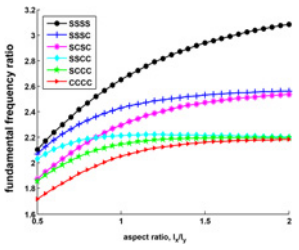

Fig. 4 *Variation of the fundamental frequency ratio with the aspect ratio of the piezoelectric nanoplate under different boundary conditions ($l_y=20$ nm, $h=1$ nm, $e_0a=0.5$ nm, $V_0=0$ V, $N_{xm}=N_{ym}=0$ N/m)*

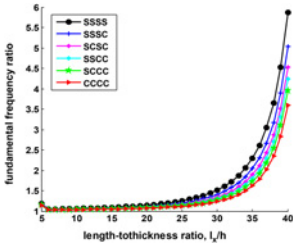

Fig. 5 *Variation of the fundamental frequency ratio with the length to thickness ratio of the piezoelectric nanoplate under different boundary conditions ($l_x=l_y=20$ nm, $e_0a=0.5$ nm, $V_0=0$ V, $N_{xm}=N_{ym}=0$ N/m)*

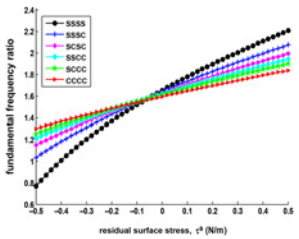

Fig. 6 *Variation of the fundamental frequency ratio with the residual surface stress of the piezoelectric nanoplate under different boundary conditions* ($l_x = l_y = 20$ *nm,* $e_0a = 0.5$ *nm,* $h = 1$ *nm,* $V_0 = 0$ *V,* $N_{xm} = N_{ym} = 0$ *N/m)*

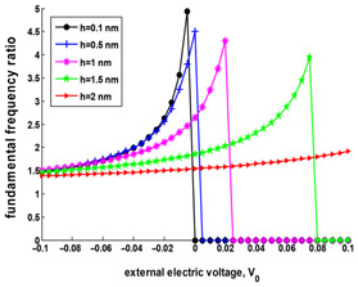

Fig. 7 *Variation of the fundamental frequency ratio with the external electric voltages of the SS piezoelectric nanoplate under different nanoplate thicknesses* ($l_x = l_y = 20$ *nm,* $e_0a = 0.5$ *nm,* $N_{xm} = N_{ym} = 0$ *N/m)*

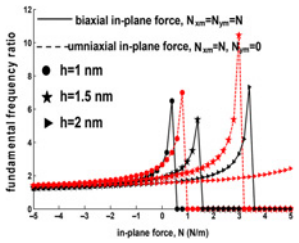

Fig. 8 *Variation of the fundamental frequency ratio with the mechanical in-plane force of the SS piezoelectric nanoplate under different nanoplate thicknesses and biaxial and uniaxial in-plane forces* ($l_x = l_y = 20$ *nm,* $e_0a = 0.5$ *nm,* $V_0 = 0$ *V)*

more solid the effect of surface layer increases, while for positive one that phenomenon is vice versa. Since in negative residual surface stress, the nanoplate has inherent softening, while for the positive one, the nanoplate has inherent stiffness. Therefore, by increasing stiffness of boundary condition, the influence of surface layer increases and decreases; respectively, for negative and positive surface residual stresses.

The effect of external electric voltage on the SS fundamental frequency ratio of piezoelectric nanoplate demonstrated in Fig. 7 versus thickness nanoplate. In this figure, the effect of mechanical in-plane force is not taken into account. It is observed that the effect of surface layer declines by augmenting thickness nanoplate. Moreover, by increasing the thickness of nanoplate the effect of external electric voltage decreases. It meant that the sudden change in curves transpires later, since the stiffness of nanoplate has been increased.

Fig. 8 shows the influences of biaxial and uniaxial mechanical forces on the SS fundamental frequency ratio of piezoelectric nanoplate for various nanoplate thicknesses. The external electric voltage is zero. It is found that by increasing biaxial and uniaxial mechanical forces, the fundamental frequency ratio raises. Thus, the effect of surface layer enhances. Moreover, for a critical value of mechanical force the out-of-plane stiffness of nanoplate

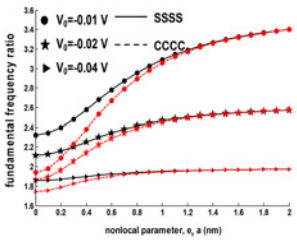

Fig. 9 *Variation of the fundamental frequency ratio with the non-local parameter of the piezoelectric nanoplate under diverse external electric voltages and boundary condition* ($l_x = l_y = 20$ *nm,* $h = 1$ *nm,* $N_{xm} = N_{ym} = 0$ *N/m)*

becomes zero. This phenomenon happens sooner for nanoplate in the case of biaxial in-plane force as compared with uniaxial one. Since in the case of biaxial, the stiffness of nanoplate is less than the case of uniaxial.

Fig. 9 represents the non-local parameter effect on the clamped and SS fundamental frequency ratio of piezoelectric nanoplates for diverse external electric voltage. It can be seen that the effect of the surface layer would increase by augmenting non-local parameter. Since the non-local parameter has inherent softening; therefore, the effect of surface layer could exhibit itself more. In addition, for the higher value of non-local small scale, the type of boundary condition is not important.

5 Conclusions: In this paper, fundamental frequency analysis of rectangular piezoelectric nanoplates via surface layers and non-local elasticity hypothesis were studied. The piezoelectric nanoplate was under mechanical and electrical in-plane forces. The governing equation of piezoelectric nanoplate was achieved via two variable refined plate theory. To solve the equations of motion, the finite difference method was employed. To verify the exactness of the finite difference solution, the governing equations of motion were tested by the Navier's solution. Result demonstrated that by augmenting the external electric voltage, biaxial, and uniaxial mechanical forces, plate aspect ratio, length to thickness ratio, residual surface stress, and non-local parameter, the influence of surface layer increased, while by increasing the nanoplate stiffness and thickness the effects of surface decreased in the fundamental frequency of piezoelectric nanoplates. Moreover, in the higher value of plate aspect ratio and length to thickness ratio, the surface layer effect was dependent on boundary condition, while for the higher value of small scale the type of boundary condition was not remarkable. In addition, for negative residual surface stress, when the boundary condition got solid, the effects of surface layer increased, while for positive one that phenomenon was inverse. The out-of-plane stiffness of nanoplate became zero sooner for biaxial mechanical forces as compared with uniaxial one. Also, that incident happened for SSSS boundary condition as compared with CCCC one.

6 References

[1] Sinha N., Wabiszewski G.E., Mahameed R., *ET AL.*: 'Piezoelectric aluminum nitride nano-electromechanical actuators', *Appl. Phys. Lett.*, 2009, **95**, p. 053106

[2] Eringen A.C., Edelen D.G.B.: 'On nonlocal elasticity', *Int. J. Eng. Sci.*, 1972, **10**, pp. 233–248

[3] Gurtin M.E., Murdoch A.I.: 'Surface stress in solids', *Int. J. Solids Struct.*, 1978, **14**, pp. 431–440

[4] Yan Z., Jiang L.Y.: 'Vibration and buckling analysis of a piezoelectric nanoplate considering surface effects and in-plane constraints', *Proc. R. Soc. A*, 2012, **468**, pp. 3458–3475

[5] Karimi M., Mirdamadi H.R., Shahidi A.R.: 'Positive and negative surface effects on the buckling and vibration of rectangular nanoplates under biaxial and shear in–plane loadings based on nonlocal elasticity theory', *J. Braz. Soc. Mech. Sci. Eng.*, 2017, **39**, pp. 1391–1404

doi: 10.1049/mnl.2017.0429

[6] Karimi M., Shahidi A.R.: 'Finite difference method for sixth order derivatives of differential equations in buckling of nanoplates due to coupled surface energy and non-local elasticity theories', *Int. J. Nano Dimens.*, 2015, **6**, pp. 525–538
[7] Karimi M., Shokrani M.H., Shahidi A.R.: 'Size-dependent free vibration analysis of rectangular nanoplates with the consideration of surface effects using finite difference method', *J. Appl. Comput. Mech.*, 2015, **1**, pp. 122–133
[8] Karimi M., Shahidi A.R.: 'Finite difference method for biaxial and uniaxial buckling of rectangular silver nanoplates resting on elastic foundations in thermal environments based on surface stress and non-local elasticity theories', *J. Solid Mech.*, 2016, **8**, pp. 719–733
[9] Kolahchi R., Hosseini H., Esmailpour M.: 'Differential cubature and quadrature-Bolotin methods for dynamic stability of embedded piezoelectric nanoplates based on visco-nonlocal-piezoelasticity theories', *Compos. Struct.*, 2016, **157**, pp. 174–186
[10] Haghshenas A., Ghorbanpour Arani A.: 'Nonlocal vibration of a piezoelectric polymeric nanoplate carrying nanoparticle via Mindlin plate theory', *Proc. I MechE C Eng. Sci.*, 2014, **228**, pp. 907–920
[11] Ke L.L., Liu C., Wang Y.S.: 'Free vibration of nonlocal piezoelectric nanoplates under various boundary conditions', *Physica E*, 2015, **66**, pp. 93–106
[12] Shimpi R.: 'Refined plate theory and its variants', *AIAA J.*, 2002, **40**, pp. 137–146
[13] Shokrani M.H., Karimi M., Tehrani M.S., *ET AL.*: 'Buckling analysis of double-orthotropic nanoplates embedded in elastic media based on non-local two-variable refined plate theory using the GDQ method', *J. Braz. Soc. Mech. Sci. Eng.*, 2016, **38**, pp. 2589–2606
[14] Karimi M., Haddad H.A., Shahidi A.R.: 'Combining surfaceeffects and non-local two variable refined plate theories on theshear/biaxial buckling and vibration of silver nanoplates', *Micro Nano Lett.*, 2015, **10**, pp. 276–281
[15] Karimi M., Mirdamadi H.R., Shahidi A.R.: 'Shear vibrationand buckling of double-layer orthotropic nanoplates based on RPT resting on elastic foundations by DQM including surface effects', *Microsyst. Technol.*, 2017, **23**, pp. 765–797
[16] Karimi M., Shahidi A.R.: 'Thermo-mechanical vibration, buckling, and bending of orthotropic graphene sheets based on nonlocal two-variable refined plate theory using finite difference method considering surface energy effects', Proc I MechE Part N: J Nanomaterials, Nanoengineering and Nanosystems, 2017, doi.: 10.1177/2397791417719970.
[17] Farajpour M.R., Rastgoo A., Farajpour A., *ET AL.*: 'Vibration of piezoelectric nanofilm-based electromechanical sensors via higher-order nonlocal strain gradient theory', *Micro Nano Lett.*, 2016, **11**, pp. 302–307
[18] Nazemizadeh M., Bakhtiari-Nejad F.: 'Size-dependent free vibration of nano/microbeams with piezo-layered actuators', *Micro Nano Lett.*, 2015, **10**, pp. 93–98
[19] Karimi M., Shahidi A.R.: 'Nonlocal, refined plate, and surface effects theories used to analyze free vibration of magnetoelectro-elastic nanoplates under thermo-mechanical and shear loadings', *Appl. Phys. A*, 2017, **123**, pp. 304, https://doi.org/10.1007/s00339-017-0828-2
[20] Karimi M., Shahidi A.R., Ziaei-Rad S.: 'Surface layer and nonlocal parameter effects on the in-phase and out-of-phase natural frequencies of a double-layer piezoelectric nanoplate under thermo-electro-mechanical loadings', *Microsyst. Technol.*, 2017, doi:10.1007/s00542-017-3395-8